Automatic Digital Garment Initialization from Sewing Patterns

ANONYMOUS AUTHOR(S)
SUBMISSION ID: PAPERS_150

(a) The initialized garment (front) (b) The initialized garment (back) (c) The simulated garment (front) (d) The simulated garment (back)

Fig. 1. A quilted coat example with 358 pattern pieces. By providing the sewing pattern and the sewing relationships for this garment, as depicted in the inset of (a), our system reliably and efficiently calculates an initialization with no folding or intersection in 17 seconds, as shown in (a) and (b). This initial setup forms the basis for a followup physics-based simulator, effortlessly producing visually stunning simulations in (c) and (d). Without our system, users would encounter substantial challenges in preparing a garment of this complexity for simulation.

The rapid advancement of digital fashion and generative AI technology calls for an automated approach to transform digital sewing patterns into well-fitted garments on human avatars. When given a sewing pattern with its associated sewing relationships, the primary challenge is to establish an initial arrangement of sewing pieces that is free from folding and intersections. This setup enables a physics-based simulator to seamlessly stitch them into a digital garment, avoiding undesirable local minima. To achieve this, we harness AI classification, heuristics, and numerical optimization. This has led to the development of an innovative hybrid system that minimizes the need for user intervention in the initialization of garment pieces. The seeding process of our system involves the training of a classification network for selecting seed pieces, followed by solving an optimization problem to determine their positions and shapes. Subsequently, an iterative selection-arrangement procedure automates the selection of pattern pieces and employs a phased initialization approach to mitigate local minima associated with numerical optimization. Our experiments confirm the reliability, efficiency, and scalability of our system when handling intricate garments with multiple layers and numerous pieces. According to our findings, 68 percent of garments can be initialized with zero user intervention, while the remaining garments can be easily corrected through user operations during post-processing.

CCS Concepts: • **Computing methodologies** → **Physical simulation**.

Additional Key Words and Phrases: Physics-based cloth simulation, numerical optimization, digital fashion, local minima, sewing pattern

ACM Reference Format:
Anonymous Author(s). 2024. Automatic Digital Garment Initialization from Sewing Patterns. *ACM Trans. Graph.* 1, 1 (January 2024), 10 pages. https://doi.org/10.1145/nnnnnnn.nnnnnnn

0730-0301/2024/1-ART $15.00
https://doi.org/10.1145/nnnnnnn.nnnnnnn

1 INTRODUCTION

With the rise of digital fashion businesses and the progress in generative AI models, digital sewing patterns have become more accessible and affordable. This advancement raises an intriguing question: how can we effortlessly convert digital sewing patterns into well-fitted digital garments on human avatars, all through a fully automated process? This capability is in high demand for a range of digital fashion and entertainment applications, as it forms a key component in the automated creation of 3D garments and characters.

Unfortunately, when presented with a sewing pattern and its sewing relationships, cloth simulation often grapples with non-uniqueness, resulting in visual artifacts primarily due to local minima. These artifacts can manifest as self-folding in Fig. 2a, cloth-body intersection in Fig. 2b, or misplaced pieces stuck outside of the body in Fig. 2c, depending on how the simulation objective is defined and optimized. To mitigate the local minima issue, a natural solution is to employ a suitable initialization. In essence, the goal of an initialization is to position the sewing pieces around the human body without folding or intersection, thus enabling the generation of visually acceptable digital garments through simulation. An intersection-free initialization is also important to simulators that rely on continuous collision detection and interior point methods [Li et al. 2020].

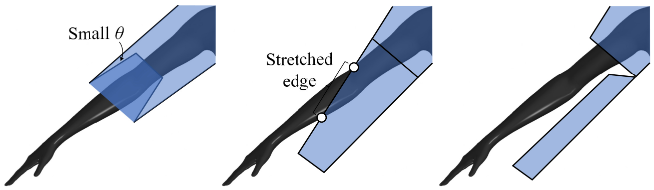

(a) A folded sleeve (b) A stretched sleeve (c) A misplaced sleeve

Fig. 2. Improper simulation outcomes of a sleeve on the body. Each outcome signifies a local minimum in the simulation problem. Ideally, clothing should be worn properly by the body with no folding or intersection.

While researchers have long acknowledged the challenge of addressing local minima in simulation, their primary focus has traditionally revolved around mitigating numerical instability [Volino and Thalmann 2000; Wang et al. 2023; Wu and Kim 2023]. In this pursuit, the complexities of establishing a suitable initialization have often been overshadowed. A relatively straightforward aspect of garment initialization involves the assignments of pattern pieces to body parts. Such assignments can be automatically extracted from pattern shapes and labels [Berthouzoz et al. 2013], or manually determined by users. However, a more complex issue emerges when trying to establish the suitable initial shape for each sewing piece without folding or intersection. While simply projecting a piece onto a pre-defined planar or cylindrical surface is adequate for basic garments, it is impractical and demands significant manual intervention when dealing with complex garments featuring small pieces, multiple layers, or asymmetric sewing configurations like shirring. Such manual intervention disrupts the smooth, automated workflow for generating digital garments in an unsupervised manner.

Assuming a digital garment is provided with the sewing pattern and all sewing relationships, we present an automatic initialization system to tackle the local minima issue in subsequent simulations. Our system is founded on a phased approach, gradually introducing pattern pieces and objective potentials into an optimization-based initialization procedure. This phased approach not only addresses the local minima but also offers unique advantages.

- It achieves high efficiency by optimizing only a small set of pattern pieces at a time.
- It conveniently resolves inter-piece intersections based on the order of piece arrangement.
- It is user-friendly and allows user intervention whenever necessary, especially if the pattern input is imperfect.

Based on this approach, we make the following contributions:

- **Seeding.** We train a classification network to automatically select the initial piece(s), referred to as the *seed*, to be arranged. Subsequently, we formulate an optimization problem to initialize the seed shape on the human body.
- **Selection.** We propose an effective heuristic function for selecting the next piece to be arranged. We also illustrate the essential criteria for simultaneously arranging multiple pieces and introduce an algorithm for automated detection and merging of these pieces.
- **Arrangement.** We formulate the arrangement of the selected piece(s) as an optimization problem. To tackle the local minima issue, we invent a phased approach by progressively adding potentials into the objective. Furthermore, we provide a set of criteria for assessing the arrangement quality. These criteria enable our system to reattempt the arrangement if it does not meet the standards.

We have implemented the proposed automatic initialization system on the CPU and tested it alongside our in-house simulation engine. Our experiments confirm that the system can handle the initialization of a diverse range of garments on various human body avatars, often necessitating minimal to no user intervention. Most garments can be initialized within a matter of seconds, and the system exhibits scalability in handling complex, multi-layered garments, including the square down coat with 358 pieces, as depicted in Fig. 1.

2 RELATED WORK

2.0.1 *Physics-based cloth simulation.*

Physics-based cloth simulation has been a significant area of research in computer graphics since the seminal work by Baraff and Witkin [1998]. Depending on the representation of cloth, cloth simulation techniques fall into three categories: spring-based [Bridson et al. 2003; Choi and Ko 2002; Liu et al. 2013], continuum-based [Narain et al. 2012; Volino et al. 2009], and yarn-based [Cirio et al. 2014; Kaldor et al. 2008, 2010]. In recent years, cloth simulation research has predominantly focused on three critical directions: modeling and characterizing the mechanical properties of cloth [Miguel et al. 2012, 2013; Sperl et al. 2022; Wang et al. 2011], effective handling of self-frictional contacts [Bridson et al. 2002; Brochu et al. 2012; Chen et al. 2023; Li et al. 2018, 2020; Ly et al. 2020; Tang et al. 2018], and enhancing simulation performance through numerical algorithms [Narain et al. 2016; Tamstorf et al. 2015; Wang and Yang 2016; Wu et al. 2020]. Like other simulation challenges, cloth simulation is notable for its issue with local minima, particularly when dealing with cloth-body collisions using repulsion potentials. While researchers have explored the impact of local minima on the stability of numerical solvers [Volino and Thalmann 2000; Wang et al. 2023; Wu and Kim 2023], there remains an uncharted domain – the existence of multiple solutions, each mathematically plausible but visually unsatisfactory for properly draped garments.

2.0.2 *Pattern design and optimization.*

In the past, researchers predominantly considered sewing pattern modeling as a tool to assist fashion manufacturing, often entailing extensive user interaction. However, in recent years, there has been a growing acknowledgment of the importance of automatic sewing pattern generation within the digital fashion and entertainment industries. Research in this field can be broadly classified into two main directions: optimizing existing sewing patterns to meet specific user-defined objectives [Bartle et al. 2016; Ly et al. 2018; Umetani et al. 2011; Wang 2018], and reconstructing sewing patterns from various garment sources, including parametric templates [Korosteleva and Lee 2021], meshes [Goto and Umetani 2021; Pietroni et al. 2022], sketches [Wang et al. 2018], 3D scans [Bang et al. 2021; Korosteleva and Lee 2022], and images [Liu et al. 2023; Yang et al. 2018].

Our system seamlessly integrates with the majority of existing automatic sewing pattern optimization and generation techniques, as they inherently provide patterns with sewing relationships that are essential for our system. Our system also benefits from pattern parsing techniques [Berthouzoz et al. 2013], which aim to automatically determine sewing relationships and piece assignments.

3 SYSTEM PIPELINE

Our system takes a sewing pattern and a human body as input and generates an initialized garment on the same body as output. It comprises three key processes as Fig. 8 shows. The first process is seeding, which uses a classification network to find the first piece(s) to be arranged and applies geometric optimization to calculate their initial shapes. If the automatically selected seed is ineffective, users can manually choose their seed. Once the system initializes the seed, it runs the selection process to find the next piece(s) and employs the arrangement process to initialize them. Compared with the others, the arrangement process is more computation-intensive. It contains three iterative steps and terminates only when the arranged shapes are satisfactory enough. The system keeps running the selection-arrangement procedure until all pieces have been arranged.

Our system operates based on the following assumptions.

- The body should be in an A-pose with both arms extended 50 degrees away from the torso.
- The pattern mesh should be resampled to achieve a uniform resolution with an average vertex distance of 20mm.
- The pattern should be associated with all sewing lines, and each sewing line should have a zero reference length.
- All of the pieces should face away from the body when incorporated into a garment worn on the body.
- All of the pieces should be oriented upright within the pattern space, matching their orientation on the garment.

Currently, we rely on preprocessing to meet these assumptions, and we anticipate that sewing patterns generated by AI models will naturally conform to these assumptions in the future.

Our system also offers postprocessing to enhance the generated garment. During this procedure, a quasistatic simulation of the entire garment is conducted using a small step size and greater repulsion strength parameters. This simulation settles the garment under the influence of gravity, eliminates remaining cloth intersections, and adjusts the body to a desired pose if it differs from the A-pose.

4 SEEDING

The seeding procedure in our system serves a dual purpose: it determines the seed piece(s) and their locations while also initializing their shapes. As mentioned in Subsection 7.1, the choice of the seed significantly influences system performance, with neck, waist, and torso pieces often proving effective seeds in our experiments. Based on this observation, we introduce both automatic and manual seeding methods in Subsection 4.1, and we discuss geometric optimization for initializing the seed in Subsection 4.2.

4.1 Seed Selection Methods

We can view seed selection as a pattern piece classification problem, with a special aim of finding the piece(s) covering the neck, waist, or torso, if the former two cannot be found. Before we present our seed selection methods, we would like to address a small issue: there can be multiple pieces covering the waist. To resolve this issue, the system selects all of the rectangular pieces with their width-to-height aspect ratios above three, and merges them if they are connected by sewing lines in a head-to-tail fashion. Doing so allows us to control the number of waist pieces to one.

4.1.1 AI-based seed selection. Given a pattern piece defined in the 2D reference pattern space, we first need to construct the encoding for determining the category it belongs to. We choose radial sampling [Liu et al. 2023] to define the shape feature of the piece. However, the shape feature alone is insufficient for determining the category, as many pieces share similar shapes but correspond to different parts on a garment. Therefore, we consider not only the piece's own shape, but also its surroundings, including both the shapes of the neighboring pieces and their sewing relationships. Since the pieces can be located anywhere within the pattern space, the length or direction of a sewing line is unimportant. Instead we extract the feature of the sewing relationship between piece $\mathcal{P}$ and its neighbor $\mathcal{P}'$ based on where their sewing boundary is located with respect to $\mathcal{P}'$:

$$S_{\mathcal{P}\to\mathcal{P}'} = \sum_{e' \in \partial\mathcal{P}'} C(e', \mathcal{P}) U(e'), \tag{1}$$

where $\partial\mathcal{P}'$ is the sewing boundary of piece $\mathcal{P}'$, $U(e')$ is the column area of $\mathcal{P}'$ under edge e' as Fig. 3a shows, and $C(\mathcal{X}, \mathcal{Y})$ is a function testing if two sets $\mathcal{X}$ and $\mathcal{Y}$ are connected by any sewing line $\mathcal{S}$:

$$C(\mathcal{X}, \mathcal{Y}) = \begin{cases} 1, & \exists x, y : x \in \mathcal{X}, y \in \mathcal{Y}, \{x, y\} \in \mathcal{S}, \\ 0, & \text{otherwise.} \end{cases} \tag{2}$$

While there exist many other ways to encode the sewing relationship, we choose Eq. 1 because it can be reused later for the piece selection heuristic (in Section 5) and it well signifies neck and waist pieces. Intuitively, when $S_{\mathcal{P}\to\mathcal{P}'}$ is large, it suggests that $\mathcal{P}$ is above $\mathcal{P}'$ on a garment[1] and $\mathcal{P}'$ is likely be to a neck or waist piece.

Our AI-based seed selection method is built upon a two-layer graph attention network [Veličković et al. 2018]. The initial layer aggregates the features of a piece and its surroundings, including both piece shape features and sewing relationship features, using an attention mechanism. The subsequent layer acts a classifier with softmax activation to predict the probability of the piece belonging to each category.

To train this classification network, we use the AdamW optimizer and we set the initial learning rate to 5×10^{-5}, the backbone to 5×10^{-6} and the weight decay to 10^{-4}. The whole training process takes 90,000 iterations and lasts 11 hours on two NVIDIA® GeForce RTX™ 4090 GPU with the batch size equal to 8. Our data set contains 23,276 labeled sewing patterns, corresponding to a wide range of garments including dresses, pants, shirts, and coats. We use 80 percent of the data for training and the rest for testing.

4.1.2 Manual seed selection. If AI-based seed selection fails to find any seed or if the seed it finds is notably incorrect, the system provides users with an option to manually select seeds. This process

[1] As mentioned previously in Section 3, we assume that all of the pieces are oriented upright in the reference pattern space.

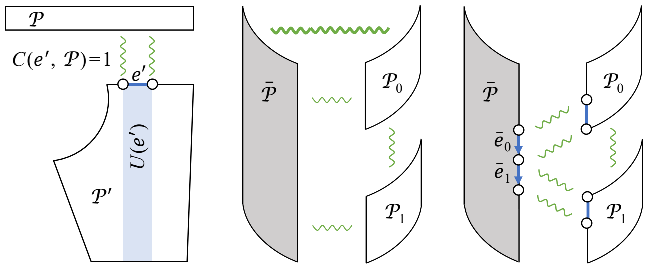

(a) Column area (b) Piece candidates (c) Merging pieces

Fig. 3. The scenarios involved in the piece selection process. Our system determines the next piece(s) to be arranged by a heuristic function, which is based on the (green) sewing relationship among the pieces.

is analogous to the arrangement procedure in other systems: users select the piece(s) and assign them to pre-defined neck, waist, or torso locations. Our system offers 15 such locations.

4.2 Seed Initialization

After selecting the seed piece(s), we would like to initialize its shape $\mathbf{x} \in \mathbb{R}^{3N}$ around the body, where N is the number of seed vertices. To achieve this, we propose to solve an optimization problem $\mathbf{x} = \arg\min F^{\text{init}}(\mathbf{x})$ with the following objective:

$$F^{\text{init}}(\mathbf{x}) = F^{\text{cent}}(\mathbf{x}) + F^{\text{up}}(\mathbf{x}) + F^{\text{dist}}(\mathbf{x}) + F^{\text{def}}(\mathbf{x}). \tag{3}$$

The centering potential, $F^{\text{cent}}(\mathbf{x}) = \frac{1}{2}k^{\text{ctr}}\left\|\mathbf{x}_c - \mathbf{x}_c^0\right\|^2$, pulls the central vertex $\mathbf{x}_c$ of the seed piece(s) toward the assigned location $\mathbf{x}_c^0$ with a strength parameter k^{ctr}. Meanwhile, the upward potential aims to maintain the seed's orientation upward:

$$F^{\text{up}}(\mathbf{x}) = -\frac{1}{2}k^{\text{up}}\sum_i \text{Sign}\left((\mathbf{r}_i - \mathbf{r}_c)^{\mathsf{T}}\begin{bmatrix} 0 \\ 1 \end{bmatrix}\right)(\mathbf{x}_i - \mathbf{x}_c)^{\mathsf{T}}\begin{bmatrix} 0 \\ 1 \\ 0 \end{bmatrix}, \tag{4}$$

where $\mathbf{r}_i$ and $\mathbf{r}_c$ are the reference vertex positions in the 2D pattern space, and k^{up} is the upward strength parameter. The body distance potential keeps the seed piece(s) close to the body:

$$F^{\text{dist}} = \frac{1}{2}k^{\text{dist}}\sum_i \max\left(\text{Sign}(\mathbf{n}(\mathbf{x}_i)\cdot\nabla\phi(\mathbf{x}_i)), 0\right)\left(\phi(\mathbf{x}_i) - D\right)^2, \tag{5}$$

in which $\mathbf{n}(\mathbf{x}_i)$ is the normal of vertex i, $\phi(\mathbf{x}_i)$ is the signed distance function of the body, D is the desired vertex-body distance, and k^{dist} is its strength parameter. Eq. 5 disables the body distance potential of vertex i if the vertex is facing toward the body. This is to prevent the seed from being stuck in a self-folded local minimum state. Finally, we need the deformation potential $F^{\text{def}}(\mathbf{x})$ to constrain the deformation of the seed shape, including both planar and bending deformations. For simplicity, we choose the spring model to limit planar deformation for each mesh edge, and the quadratic model [Bergou et al. 2006] to limit bending deformation for each dihedral edge. Other deformation models can also be effective in this context.

We use an iterative solver to solve this optimization problem. Please refer to Section 7 for solver and parameter details.

5 PIECE SELECTION

Given a set of pattern pieces already being arranged on the body, we are now faced with the task of determining the next piece(s) for arrangement. This process is pivotal, as it not only influences the quality of the final result, but also dictates how the system handles inter-piece intersections in Subsection 6.3. In this section, we will first introduce the heuristic score function, which helps us evaluate and select an individual piece. Following that, we will explore the importance of arranging multiple pieces simultaneously and our approach to selecting them.

5.1 Single Piece Selection

Let's first discuss the selection of a single piece. We propose the following heuristic to choose a piece $\mathcal{P}$ with the highest score:

$$H(\mathcal{P}) = \frac{\sum_{e\in\partial\mathcal{P}} C(e,\bar{\mathcal{P}})L_e^0}{\sum_{e\in\partial\mathcal{P}} L_e^0} + s_a A(\mathcal{P}) + s_b S_{\bar{\mathcal{P}}\to\mathcal{P}}, \tag{6}$$

in which $\bar{\mathcal{P}}$ is the set of already arranged pieces, L_e^0 is the reference length of edge e, $A(\mathcal{P})$ is the reference area of piece $\mathcal{P}$, $S_{\bar{\mathcal{P}}\to\mathcal{P}}$ is the sewing relationship score in Eq. 1, and s_a and s_b are two weight variables. In Eq. 6, the first term gives precedence to the pieces whose sewing boundaries are mostly determined by $\bar{\mathcal{P}}$ already. The second term prioritizes the arrangement of large pieces. The third term underscores the importance of selecting pieces that can be well supported from the top, such as $\mathcal{P}_0$ with thickened sewing lines on the top in Fig. 3b. Without this term, the system may opt for $\mathcal{P}_1$, which could sag excessively under gravity during shape refinement (in Subsection 6.3), due to missing support from the top.

5.2 Multiple Piece Selection

In practice, it is necessary to arrange multiple pieces simultaneously for two compelling reasons.

The first reason arises when a single piece must be intentionally divided into multiple components, often due to the use of different fabrics, such as the trench coat in Fig 10o. Arranging these pieces consecutively could result in an improper fit to the corresponding body part. To address this challenge, we need to determine whether multiple pieces can be selected and arranged as a unified whole. This determination involves testing whether the sewing boundaries of adjacent piece candidates smoothly connect on $\bar{\mathcal{P}}$, as demonstrated by the two edges $\bar{e}_0$ and $\bar{e}_1$ in Fig. 3c. If this smooth connection is confirmed, we treat these pieces as part of a larger, combined piece. Subsequently, we calculate the heuristic score for this amalgamated piece, similar to other individual pieces, and decide whether it should be selected next, as described in Subsection 5.1.

The second reason is related to parallelization. According to Section 7, on average, each piece comprises just 197 vertices, with over half of the pieces containing fewer than 100 vertices. Sequencing such small pieces one after another would not fully leverage the power of parallel processing. To address this challenge, we employ the following approach: we iteratively select additional pieces using the aforementioned process until the total number of vertices in the selected set reaches a specified cap, which, in our system, is set at 1,024. Our experiments demonstrate that this practice reduces the computational time by 60 to 80 percent.

6 PIECE ARRANGEMENT

We formulate the arrangement of the newly selected piece(s) as an optimization problem with the following objective function:

$$F(\mathbf{x}) = F^{\text{def}}(\mathbf{x}) + F^{\text{sew}}(\mathbf{x}) + F^{\text{ext}}(\mathbf{x}) + F^{\text{body}}(\mathbf{x}) + F^{\text{self}}(\mathbf{x}). \quad (7)$$

This objective shares the same deformation potential, as described in Eq. 3. However, it operates within a distinct problem domain and incorporates additional potentials. Before discussing these differences, it is important to note that this optimization is prone to local minima issues if solved immediately, as illustrated in Fig. 5a. To overcome this challenge, we employ a phased approach, gradually introducing new potentials into the system over three steps.

6.1 Initial Alignment

Let $\bar{\mathcal{P}}$ be the set of arranged pieces and $\mathcal{P}$ be the selected piece(s). We want to make an initial alignment of $\mathcal{P}$ to $\bar{\mathcal{P}}$ first, without considering body or self intersection. To do so, we initialize $\mathcal{P}$ by applying an affine transformation $\left\{\mathbf{t}, \mathbf{A} \,\middle|\, \mathbf{t} \in \mathbb{R}^3, \mathbf{A} \in \mathbb{R}^{3\times 2}\right\}$, which minimizes the sewing gap between $\mathcal{P}$ and $\bar{\mathcal{P}}$:

$$\{\mathbf{t}, \mathbf{A}\} = \arg\min \sum_{\{i,j\}\in\mathcal{S}, i\in\mathcal{P}, j\in\bar{\mathcal{P}}} \left\|\mathbf{t} + \mathbf{A}\mathbf{r}_i - \mathbf{x}_j\right\|^2, \quad (8)$$

where $\{i, j\}$ is a sewing pair between $\mathcal{P}$ and $\bar{\mathcal{P}}$, $\mathbf{r}_i$ is the 2D pattern position of vertex i, and $\mathbf{x}_j$ is the 3D garment position of vertex j. To solve Eq. 8, we use its closed-form solution [Müller et al. 2005], which requires at least two non-trivial sewing lines between $\mathcal{P}$ and $\bar{\mathcal{P}}$. If that is not true, we simply set $\mathbf{A} = [\mathbf{I} \quad \mathbf{0}]^{\mathsf{T}}$. Once we transform $\mathcal{P}$, we optimize its shape by minimizing a truncated objective function: $F(\mathbf{x}) = F^{\text{sew}}(\mathbf{x}) + F^{\text{def}}(\mathbf{x}) + F^{\text{ext}}(\mathbf{x})$. Here we define the sewing potential by quadratic energies:

$$F^{\text{sew}}(\mathbf{x}) = \frac{1}{2}k^{\text{sew}} \sum_{\{i,j\}\in\mathcal{S}} \left\|\mathbf{x}_i - \mathbf{x}_j\right\|^2, \quad (9)$$

where k^{sew} is the sewing strength parameter. We define the external potential as:

$$F^{\text{ext}}(\mathbf{x}) = \frac{1}{2}k^{\text{fix}} \sum_{i\in\bar{\mathcal{P}}} \left\|\mathbf{x}_i - \mathbf{x}_i^0\right\|^2 - k^{\text{const}} \sum_{i\in\mathcal{P}} \mathbf{x}_i^{\mathsf{T}} \frac{\mathbf{f}}{\|\mathbf{f}\|}, \quad (10)$$

where k^{fix} and k^{const} are two strength parameters. In Eq. 10, the first term tries to prevent each vertex i of piece $\bar{\mathcal{P}}$ from leaving its originally arranged position $\mathbf{x}_i^0$, while the second term pushes each vertex of $\mathcal{P}$ in a constant direction: $\mathbf{f} = \sum_{\{i,j,k\}} \left(\mathbf{x}_i + \mathbf{x}_j - 2\mathbf{x}_k\right)$, in which i, j, and k are the vertices of a sewing boundary triangle on $\bar{\mathcal{P}}$, as shown in Fig. 4a. Without the second term, $\mathcal{P}$ may get stuck in the opposite side of the sewing boundary.

To smooth the boundary between $\mathcal{P}$ and $\bar{\mathcal{P}}$, we define the problem domain $\mathbf{x}$ as the union of $\mathcal{P}$ and the two-ring sewing boundary neighborhood on $\bar{\mathcal{P}}$, as Fig. 4a shows. We also integrate sewing edge pairs into the dihedral edge set $\mathcal{E}'$, if the two sewing edges (in blue) are topologically consistent. We incorporate each potential into the total objective, if all of the relevant vertices exist in $\mathbf{x}$. To help reduce the local minima issue related to bending deformation, we intentionally increase the magnitude of bending resistance. The results of a selected sleeve after affine transformation and initial alignment are shown in Fig. 5b and 5c, respectively.

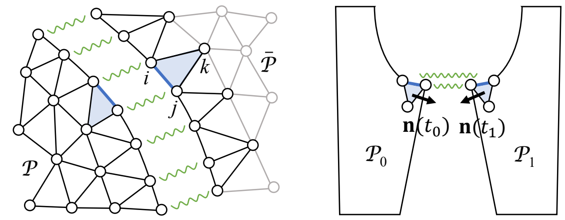

(a) The boundary between $\mathcal{P}$ and $\bar{\mathcal{P}}$ (b) The boundary between leg pieces

Fig. 4. The sewing boundaries. To smooth the sewing boundary, we add the vertices within the two-ring neighborhood on $\bar{\mathcal{P}}$ into the problem domain, as depicted in (a). However, we cannot improve the smoothness near the crotch, as the leg pieces are supposed to face against each other as (b) shows.

6.2 Body Intersection Removal

The body intersection removal step resembles the initial alignment step, but with additional repulsion potentials:

$$F^{\text{body}}(\mathbf{x}) = \frac{1}{2}k^{\text{body}} \sum_i \left(\min\left(\phi(\mathbf{x}_i) - \epsilon, 0\right)\right)^2, \quad (11)$$

where $\phi(\mathbf{x}_i)$ is the signed distance function of the body, k^{body} is the body repulsion strength parameter, and ϵ is the repulsion buffer distance. In our system, $\epsilon = 4\text{mm}$.

If we activate the body repulsion potentials for all of the vertices immediately, the simulation could easily be trapped in local minima with body intersections, as evident in Fig. 5d, since the initial alignment of $\mathcal{P}$ does not account for body collisions. To address this issue, we recognize that the sewing boundary vertices connected to $\bar{\mathcal{P}}$ do not experience the intersection issue. Therefore, we incrementally activate the potentials of the piece vertices through a flood fill process initiated from the sewing boundary. This method mimics the real-world process of donning a garment: as the body extends, the clothing untangles and covers the body, as Fig. 5e shows.

6.3 Shape Refinement

Our last aim is to resolve self-intersections of cloth and make further refinements to the garment shape.

There are two types of self-intersections: intra-piece intersections and inter-piece intersections. Since existing untangling algorithms [Baraff et al. 2003; Volino and Magnenat-Thalmann 2006] are expensive and cannot guarantee the removal of inter-piece intersections, we focus on addressing them exclusively. But instead of developing new untangling algorithms as in [Buffet et al. 2019], we take a simple approach. We assume that piece $\mathcal{P}$ is located outside of the already arranged pieces, and we apply a repulsion potential to every vertex $i \in \mathcal{P}$ and its closest triangle $t = \{j, k, l\}$ within $\bar{\mathcal{P}}$:

$$F^{\text{self}}(\mathbf{x}) = \frac{1}{2}k^{\text{self}} \sum_{i\in\mathcal{P}} \left(\min\left((\mathbf{x}_i - \mathbf{x}_j)\cdot\mathbf{n}(t) - \epsilon, 0\right)\right)^2, \quad (12)$$

in which $\mathbf{n}(t)$ is the constant normal of triangle t, k^{self} is the self repulsion strength parameter, and ϵ is the same buffer distance used in Eq. 11. One advantage of our approach is that we do not require the complete elimination of intersections during the arrangement process, which would necessitate a large k^{self} and significant computational time. Instead, we can address any remaining intersection in

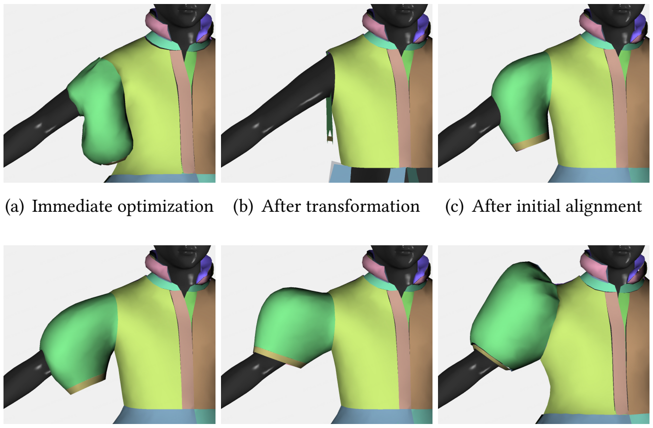

(a) Immediate optimization (b) After transformation (c) After initial alignment

(d) After quick repulsion (e) After phased repulsion (f) After shape refinement

Fig. 5. The results of a sleeve in the puff-sleeve dress example. To arrange selected piece(s), we adopt a phased approach that gradually adds new potentials into the objective, as depicted in (b), (c), (e), and (f). Without this approach, the optimization can lead to local minima, as in (a) and (d).

post-processing, as discussed in Section 3. This is possible because the inside-outside relationship among pieces remains unchanged once it is determined by the piece arrangement order.

During shape refinement, our optimization occurs in two phases. In the first phase, we introduce self-repulsion potentials into the objective and reduce bending resistance to its normal value, allowing cloth to bend more readily. In the second phase, we replace the second term of F^{ext} by gravitational potential, so that cloth can drape naturally. Furthermore, we expand the problem domain beyond the two-ring sewing boundary neighborhood of $\bar{\mathcal{P}}$ and fix the vertices on $\bar{\mathcal{P}}$ only if they are away from the boundary. This expansion helps refine the garment shape near the sewing boundary, especially for shirring as Fig. 5f shows. In our system, we define the expanded domain as the 16-ring neighborhood from the sewing boundary.

6.4 Termination Conditions

After the completion of all three steps, we assess the quality of the arrangement based on the following criteria:

$$\theta_{\text{in}} = \min_{\{t_0,t_1\}\in\mathcal{N}} \mathbf{n}(t_0)\cdot\mathbf{n}(t_1),\ \ \theta_{\text{out}} = \min_{\{t_0,t_1\}\in\mathcal{B}} \mathbf{n}(t_0)\cdot\mathbf{n}(t_1),$$
$$s_{\text{max}} = \max_{\{i,j\}\in\mathcal{E}} \left(\left\|\mathbf{x}_i - \mathbf{x}_j\right\| - L^0_{ij}\right), \tag{13}$$

where $\mathbf{n}(t)$ is the normal of triangle t, $\mathcal{N}$ is the set of neighboring triangles, and $\mathcal{B}$ is the set of boundary triangles adjacent to each other after sewing. Intuitively, θ_{in} assesses whether a piece has been excessively folded, θ_{out} examines if two adjacent pieces have been excessively folded along their boundary, and s_{max} checks for significant stretching of any spring edge. When $\theta_{\text{in}} < \theta^0_{\text{in}}$, it suggests a piece may be folded or intersected, and we simply reiterate the entire arrangement process until the piece is flattened. However, in the case of $\theta_{\text{out}} < \theta^0_{\text{out}}$, repetitions may not necessarily increase θ_{out}, as observed in scenarios such as the crotch formed by leg pieces in Fig. 4b. Therefore, we redo the arrangement process only once when $\theta_{\text{out}} < \theta^0_{\text{out}}$. Finally, if $s_{\text{max}} > s^0_{\text{max}}$, it implies a piece has been overly stretched due to cloth-body intersections as Fig. 2b shows. This issue may result from insufficient piece selection or the arrangement process itself. As we cannot immediately determine the primary cause, we include the neighboring pieces of the currently selected one into the set once, and then repeat the arrangement process. The system concludes the arrangement process when no further repetition is necessary, according to the criteria.

The computational cost of the arrangement process relies on the number of iterations spent by the solver at each step, and the initial alignment step is of particular importance to the final arrangement quality. Since most pieces can be arranged during the first arrangement with a few initial alignment iterations, we intentionally reduce the number of initial alignment iterations for less cost. The numbers of iterations spent at each step are listed in Fig. 8.

7 RESULTS AND DISCUSSIONS

We implement our system exclusively on the CPU to ensure compatibility across multiple hardware platforms. The implementation of our system is solver-independent for optimization and simulation tasks. In practice, we employ a solver based on the parallelized gradient descent method with Jacobi preconditioning and Chebyshev acceleration [Wang and Yang 2016], utilizing a fixed step size (with $\alpha = 0.4$) and a fixed spectral radius (with $\rho = 0.9994$). While projective dynamics [Bouaziz et al. 2014] could also be used for initial alignment, we have found it less capable of handling phased intersection removal, as discussed in Section 6.2 and 6.3.

We assess the performance of our system using 21 sewing patterns designed for six body types. These patterns encompass various garment types, including pants, dresses, coats, and shirts. Depending on the pattern design, the number of vertices (after resampling) ranges from 1.5K to 23K, and the number of pieces varies from 7 to 358. On average, each piece contains 197 vertices, and about 52 percent of the pieces contains 100 vertices or fewer.

7.1 Efficiency Evaluation

We evaluate the efficiency of our system on a workstation with an Intel® Core™ i9-13900K 3.00 GHz CPU. Fig. 6a provides a breakdown of the computational time dedicated to the puff-sleeve dress example. Among the processes involved, the arrangement process is the most expensive one. Further analysis within it reveals that the shape refinement step contributes the most to the cost.

According to Subsection 6.4, if the first pass fails to meet the criteria, we revisit the piece arrangement process and increase the number of iterations. Figure 6a illustrates that this practice nearly doubles the computational cost when the system revisits the process twice in this example. Fortunately, our experiments, summarized in Figure 6b, show that 52 percent of the examples require zero or one revisit, and only 10 percent of the examples need more than two revisits. Consequently, our system can process the majority of the examples within 10 seconds as Figure 6c shows.

Seed selection is pivotal in determining the number of revisits. In general, using better and more seeds can considerably reduce the need for revisits, associated computational costs, and even the occurrence of artifacts, as further discussed in Subsection 7.2. However, evaluating seed quality can be challenging without running

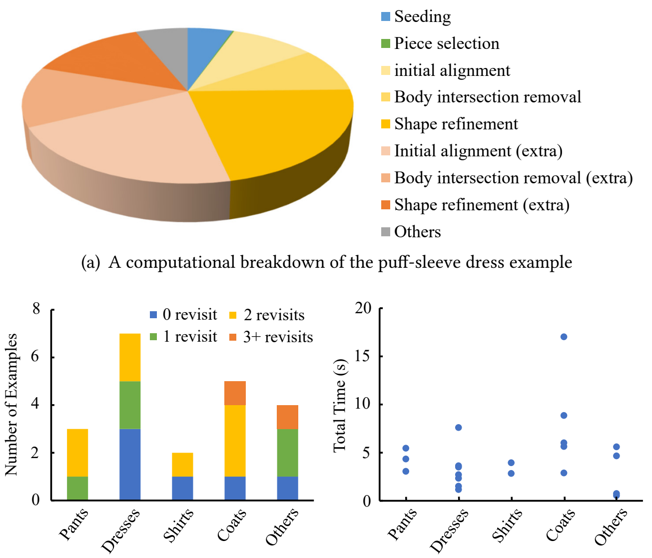

(a) A computational breakdown of the puff-sleeve dress example

(b) The examples with revisits

(c) The total computational times

Fig. 6. The charts depicting the number of revisits and the time spent for each example. These visuals establish a clear correlation between the number of revisits and the computational time. It also highlights the system's efficiency, showing high variability when processing dresses and coats.

the whole system at the first place. To ensure a fair assessment that mirrors real-world usage cases, we report performance using the very first effective seed in our experiments.

7.2 Failure Evaluation

The system successfully initializes a garment, if the whole process involves no user intervention and the result contains no obvious artifact. In this regard, the system can fail for two reasons.

First, the system can fail due to ineffective seeding. According to our data set, 86 percent of the garments contain neck or waist pieces; and according to Fig. 7a, the detection rate of a neck or waist piece is about 96 percent, while the detection rate of a body piece is 90 percent. Therefore, the likelihood of automatically finding a neck, waist, or body piece for each garment is around 95 percent.

Even if such pieces are found, they may still be ineffective and the initialization may run into major artifacts, especially if the garment is complex. Unfortunately we are unable to know this without running the system. According to our experiment, two out of 21 garments, the quilted coat in Fig. 1 and the slip dress in Fig. 10i, suffer from this issue and need manual seed re-selection.

Second, although the initialized result contains no major artifact, it may contain minor artifacts, including inter-piece intersection, wrongly located piece, and intra-piece intersection shown in Fig. 9. According to our experiments in Fig. 7b, 81 percent of the garments can be initialized with no minor artifact. Among these artifacts, inter-piece intersection is probably the simplest as it is due to an incorrect arrangement order. For instance, suppose that $\mathcal{P}_a$ and $\mathcal{P}_c$ are two connected pieces and $\mathcal{P}_b$ overlaps with them. When the order is $\mathcal{P}_a \leftarrow \mathcal{P}_b \leftarrow \mathcal{P}_c$, $\mathcal{P}_b$ would inevitably intersect with $\mathcal{P}_a$ or

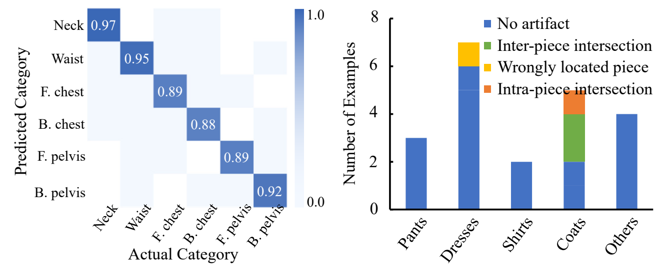

(a) The normalized confusion matrix

(b) The examples with minor artifacts

Fig. 7. Failure statistics. Our system may fail to automatically initialize garments with no obvious artifact. These charts visualize the likelihood for the system to fail during seeding and selection-arrangement procedures.

$\mathcal{P}_c$. To resolve this artifact, users can rearrange the order and redo simulation. The other artifacts can be more complex and require extensive user intervention, which is beyond the scope of this work.

Overall, given automatically selected seeds, our system correctly initializes 15 out of 21 garments with no user invention. Since the seed detection rate is around 95 percent, we anticipate the success rate of our system to be around 68 percent.

7.3 Limitations

According to Subsection 3, our system has specific requirements for body and pattern inputs. When these requirements are not met, the system may experience inefficiency or failures. Even with the requirements met, ineffective seeding, especially if the pattern misses neck, waist or body pieces, can cause the system to fail to work automatically. After the system arranges the garment, the initialized shape may still contain minor artifacts as shown in Subsection 7.2, some of which can be resolved by simple user intervention. Our system, using downsampled mesh resolution and signed distance function, does not account for cloth intersections with detailed body parts such as finger tips and hair strands. Finally, it is intriguing to know if the system can handle garments designed for humanoid and animal bodies, as we have not carried out such tests yet.

8 CONCLUSIONS AND FUTURE WORK

We present an automatic garment initialization system, which serves as the basis for automatic digital garment creation. The effectiveness of our system hinges on the assumption that the sewing relationships provide sufficient guidance for phased initialization of each pattern piece. But this assumption also implies that the system's automation relies on the choice of initial seeds and the arrangement order, which is not guaranteed to be optimal in all cases.

In the future, we plan to validate our system with additional garment cases and diverse human body avatars, with a primary focus on improving its reliability and efficiency. We have a strong interest in leveraging AI models to reduce the system's dependency on seed selection and arrangement order. Additionally, we aim to refine the system to eliminate the requirement for sewing patterns to include complete sewing relationships. This change is particularly important as it eases the burden on digital pattern makers and pattern generation algorithms.

REFERENCES

Seungbae Bang, Maria Korosteleva, and Sung-Hee Lee. 2021. Estimating Garment Patterns from Static Scan Data. *Comput. Graph. Forum* 40, 6 (Sept. 2021), 273–287.

David Baraff and Andrew Witkin. 1998. Large Steps in Cloth Simulation. In *Proceedings of SIGGRAPH 98 (Computer Graphics Proceedings, Annual Conference Series)*, Eugene Fiume (Ed.). ACM, 43–54.

David Baraff, Andrew Witkin, and Michael Kass. 2003. Untangling Cloth. *ACM Trans. Graph. (SIGGRAPH)* 22, 3 (July 2003), 862–870.

Aric Bartle, Alla Sheffer, Vladimir G. Kim, Danny M. Kaufman, Nicholas Vining, and Floraine Berthouzoz. 2016. Physics-Driven Pattern Adjustment for Direct 3D Garment Editing. *ACM Trans. Graph. (SIGGRAPH)* 35, 4, Article 50 (July 2016), 11 pages.

Miklos Bergou, Max Wardetzky, David Harmon, Denis Zorin, and Eitan Grinspun. 2006. A Quadratic Bending Model for Inextensible Surfaces. In *Proceedings of SGP*. 227–230.

Floraine Berthouzoz, Akash Garg, Danny M. Kaufman, Eitan Grinspun, and Maneesh Agrawala. 2013. Parsing Sewing Patterns into 3D Garments. *ACM Trans. Graph. (SIGGRAPH)* 32, 4, Article 85 (July 2013), 12 pages.

Sofien Bouaziz, Sebastian Martin, Tiantian Liu, Ladislav Kavan, and Mark Pauly. 2014. Projective Dynamics: Fusing Constraint Projections for Fast Simulation. *ACM Trans. Graph. (SIGGRAPH)* 33, 4, Article 154 (July 2014), 11 pages.

Robert Bridson, Ronald Fedkiw, and John Anderson. 2002. Robust Treatment of Collisions, Contact and Friction for Cloth Animation. *ACM Trans. Graph. (SIGGRAPH)* 21, 3 (July 2002), 594–603.

Robert Bridson, Sebastian Marino, and Ronald Fedkiw. 2003. Simulation of Clothing with Folds and Wrinkles. In *Proceedings of SCA*. 28–36.

Tyson Brochu, Essex Edwards, and Robert Bridson. 2012. Efficient Geometrically Exact Continuous Collision Detection. *ACM Trans. Graph. (SIGGRAPH)* 31, 4 (July 2012), 96:1–96:7.

Thomas Buffet, Damien Rohmer, Loïc Barthe, Laurence Boissieux, and Marie-Paule Cani. 2019. Implicit Untangling: A Robust Solution for Modeling Layered Clothing. *ACM Trans. Graph. (SIGGRAPH)* 38, 4 (2019).

Yunuo Chen, Tianyi Xie, Cem Yuksel, Danny Kaufman, Yin Yang, Chenfanfu Jiang, and Minchen Li. 2023. Multi-Layer Thick Shells. In *ACM SIGGRAPH 2023 Conference Proceedings* (Los Angeles, CA, USA) *(SIGGRAPH '23)*. Article 25, 9 pages.

Kwang-Jin Choi and Hyeong-Seok Ko. 2002. Stable but Responsive Cloth. *ACM Trans. Graph. (SIGGRAPH)* 21, 3 (July 2002), 604–611.

Gabriel Cirio, Jorge Lopez-Moreno, David Miraut, and Miguel A. Otaduy. 2014. Yarn-Level Simulation of Woven Cloth. *ACM Trans. Graph. (SIGGRAPH Asia)* 33, 6, Article 207 (Nov. 2014), 11 pages.

Chihiro Goto and Nobuyuki Umetani. 2021. Data-Driven Garment Pattern Estimation from 3D Geometries. In *Eurographics 2021 - Short Papers*. The Eurographics Association.

Jonathan M. Kaldor, Doug L. James, and Steve Marschner. 2008. Simulating Knitted Cloth at the Yarn Level. *ACM Trans. Graph. (SIGGRAPH)* 27, 3, Article 65 (Aug. 2008), 9 pages.

Jonathan M. Kaldor, Doug L. James, and Steve Marschner. 2010. Efficient Yarn-Based Cloth with Adaptive Contact Linearization. *ACM Trans. Graph. (SIGGRAPH)* 29, 4, Article 105 (July 2010), 10 pages.

Maria Korosteleva and Sung-Hee Lee. 2021. Generating Datasets of 3D Garments with Sewing Patterns. In *Proceedings of NeurIPS*, J. Vanschoren and S. Yeung (Eds.), Vol. 1.

Maria Korosteleva and Sung-Hee Lee. 2022. NeuralTailor: Reconstructing Sewing Pattern Structures from 3D Point Clouds of Garments. *ACM Trans. Graph. (SIGGRAPH)* 41, 4, Article 158 (jul 2022), 16 pages.

Jie Li, Gilles Daviet, Rahul Narain, Florence Bertails-Descoubes, Matthew Overby, George E. Brown, and Laurence Boissieux. 2018. An Implicit Frictional Contact Solver for Adaptive Cloth Simulation. *ACM Trans. Graph. (SIGGRAPH)* 37, 4, Article 52 (July 2018), 15 pages.

Minchen Li, Zachary Ferguson, Teseo Schneider, Timothy Langlois, Denis Zorin, Daniele Panozzo, Chenfanfu Jiang, and Danny M. Kaufman. 2020. Incremental Potential Contact: Intersection- and Inversion-Free Large Deformation Dynamics. *ACM Trans. Graph. (SIGGRAPH)* 39, 4 (July 2020).

Lijuan Liu, Xiangyu Xu, Zhijie Lin, Jiabin Liang, and Shuicheng Yan. 2023. Towards Garment Sewing Pattern Reconstruction from a Single Image. *ACM Trans. Graph. (SIGGRAPH Asia)* 42, 6 (Dec. 2023).

Tiantian Liu, Adam W. Bargteil, James F. O'Brien, and Ladislav Kavan. 2013. Fast Simulation of Mass-Spring Systems. *ACM Trans. Graph. (SIGGRAPH Asia)* 32, 6, Article 214 (Nov. 2013), 7 pages.

Mickaël Ly, Romain Casati, Florence Bertails-Descoubes, Mélina Skouras, and Laurence Boissieux. 2018. Inverse Elastic Shell Design with Contact and Friction. *ACM Trans. Graph. (SIGGRAPH Asia)* 37, 6, Article 201 (dec 2018), 16 pages.

Mickaël Ly, Jean Jouve, Laurence Boissieux, and Florence Bertails-Descoubes. 2020. Projective Dynamics with Dry Frictional Contact. *ACM Trans. Graph. (SIGGRAPH)* 39, 4, Article 57 (July 2020), 8 pages.

Eder Miguel, Derek Bradley, Bernhard Thomaszewski, Bernd Bickel, Wojciech Matusik, Miguel A. Otaduy, and Steve Marschner. 2012. Data-Driven Estimation of Cloth Simulation Models. *Comput. Graph. Forum (Eurographics)* 31, 2 (May 2012).

Eder Miguel, Rasmus Tamstorf, Derek Bradley, Sara C. Schvartzman, Bernhard Thomaszewski, Bernd Bickel, Wojciech Matusik, Steve Marschner, and Miguel A. Otaduy. 2013. Modeling and Estimation of Internal Friction in Cloth. *ACM Trans. Graph. (SIGGRAPH Asia)* 32, 6, Article 212 (Nov. 2013), 10 pages.

Matthias Müller, Bruno Heidelberger, Matthias Teschner, and Markus Gross. 2005. Meshless Deformations Based on Shape Matching. *ACM Trans. Graph. (SIGGRAPH)* 24, 3 (July 2005), 471–478.

Rahul Narain, Matthew Overby, and George E. Brown. 2016. ADMM ⊇ Projective Dynamics: Fast Simulation of General Constitutive Models. In *Proceedings of SCA*. 21–28.

Rahul Narain, Armin Samii, and James F. O'Brien. 2012. Adaptive Anisotropic Remeshing for Cloth Simulation. *ACM Trans. Graph. (SIGGRAPH Asia)* 31, 6, Article 152 (Nov. 2012), 10 pages.

Nico Pietroni, Corentin Dumery, Raphael Falque, Mark Liu, Teresa Vidal-Calleja, and Olga Sorkine-Hornung. 2022. Computational Pattern Making from 3D Garment Models. *ACM Trans. Graph. (SIGGRAPH)* 41, 4, Article 157 (jul 2022), 14 pages.

Georg Sperl, Rosa M. Sánchez-Banderas, Manwen Li, Chris Wojtan, and Miguel A. Otaduy. 2022. Estimation of Yarn-Level Simulation Models for Production Fabrics. *ACM Trans. Graph. (SIGGRAPH)* 41, 4, Article 65 (July 2022), 15 pages.

Rasmus Tamstorf, Toby Jones, and Stephen F. McCormick. 2015. Smoothed Aggregation Multigrid for Cloth Simulation. *ACM Trans. Graph. (SIGGRAPH Asia)* 34, 6, Article 245 (Oct. 2015), 13 pages.

Min Tang, tongtong wang, Zhongyuan Liu, Ruofeng Tong, and Dinesh Manocha. 2018. I-Cloth: Incremental Collision Handling for GPU-Based Interactive Cloth Simulation. *ACM Trans. Graph. (SIGGRAPH Asia)* 37, 6, Article 204 (Dec. 2018), 10 pages.

Nobuyuki Umetani, Danny M. Kaufman, Takeo Igarashi, and Eitan Grinspun. 2011. Sensitive Couture for Interactive Garment Modeling and Editing. *ACM Trans. Graph. (SIGGRAPH)* 30, 4, Article 90 (July 2011), 12 pages.

Petar Veličković, Guillem Cucurull, Arantxa Casanova, Adriana Romero, Pietro Liò, and Yoshua Bengio. 2018. Graph Attention Networks. In *International Conference on Learning Representations*. 1–12.

Pascal Volino and Nadia Magnenat-Thalmann. 2006. Resolving Surface Collisions through Intersection Contour Minimization. *ACM Trans. Graph. (SIGGRAPH)* 25 (July 2006), 1154–1159. Issue 3.

Pascal Volino, Nadia Magnenat-Thalmann, and Francois Faure. 2009. A Simple Approach to Nonlinear Tensile Stiffness for Accurate Cloth Simulation. *ACM Trans. Graph.* 28, 4, Article 105 (Sept. 2009), 16 pages.

Pascal Volino and Nadia Magnenat Thalmann. 2000. Implementing Fast Cloth Simulation with Collision Response. In *Proceedings of CGI*. 257.

Huamin Wang. 2018. Rule-Free Sewing Pattern Adjustment with Precision and Efficiency. *ACM Trans. Graph. (SIGGRAPH)* 37, 4, Article 53 (July 2018), 13 pages.

Huamin Wang, James F. O'Brien, and Ravi Ramamoorthi. 2011. Data-Driven Elastic Models for Cloth: Modeling and Measurement. *ACM Trans. Graph. (SIGGRAPH)* 30, 4, Article 71 (July 2011), 9 pages.

Huamin Wang and Yin Yang. 2016. Descent Methods for Elastic Body Simulation on the GPU. *ACM Trans. Graph. (SIGGRAPH Asia)* 35, 6, Article 212 (Nov. 2016), 10 pages.

Tuanfeng Y. Wang, Duygu Ceylan, Jovan Popović, and Niloy J. Mitra. 2018. Learning a Shared Shape Space for Multimodal Garment Design. *ACM Trans. Graph. (SIGGRAPH Asia)* 37, 6, Article 203 (Dec. 2018), 13 pages.

Zhendong Wang, Yin Yang, and Huamin Wang. 2023. Stable Discrete Bending by Analytic Eigensystem and Adaptive Orthotropic Geometric Stiffness. *ACM Trans. Graph. (SIGGRAPH Asia)* 42, 6, Article 183 (Dec. 2023), 16 pages.

Haomiao Wu and Theodore Kim. 2023. An Eigenanalysis of Angle-Based Deformation Energies. *Proc. ACM Comput. Graph. Interact. Tech. (SCA)* 6, 3, Article 40 (Aug. 2023), 19 pages.

Longhua Wu, Botao Wu, Yin Yang, and Huamin Wang. 2020. A Safe and Fast Repulsion Method for GPU-Based Cloth Self Collisions. *ACM Trans. Graph.* 40, 1, Article 5 (Dec. 2020), 18 pages.

Shan Yang, Zherong Pan, Tanya Amert, Ke Wang, Licheng Yu, Tamara Berg, and Ming C. Lin. 2018. Physics-Inspired Garment Recovery from a Single-View Image. *ACM Trans. Graph.* 37, 5, Article 170 (nov 2018), 14 pages.

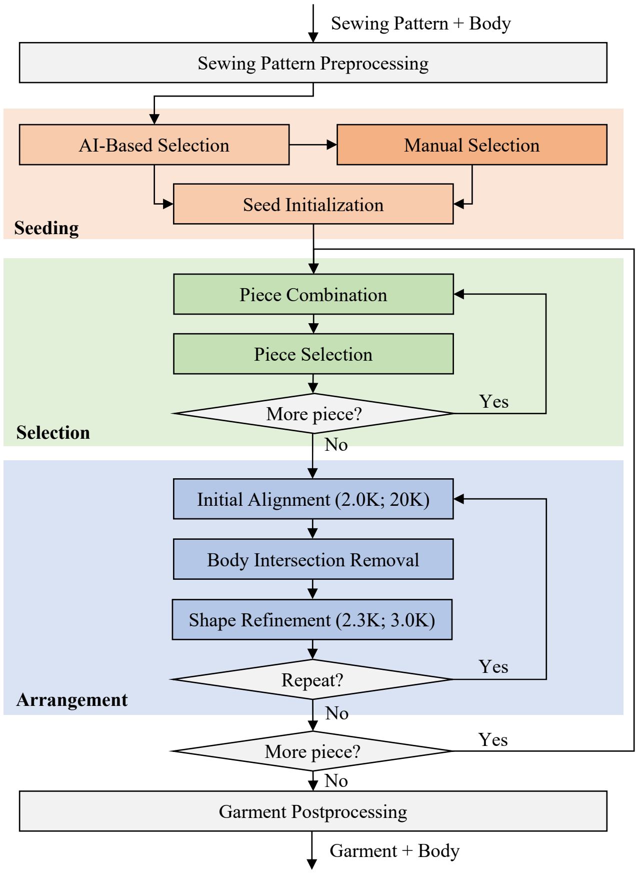

Fig. 8. The system pipeline. Our system consists of three key processes, with its core being a selection-arrangement procedure that sequentially arranges pattern pieces until none remains. During this procedure, the system may visit its steps multiple times to achieve higher parallelization and improved result quality. The numbers in the brackets are the numbers of solver iterations allocated to each step in the first and subsequent visits.

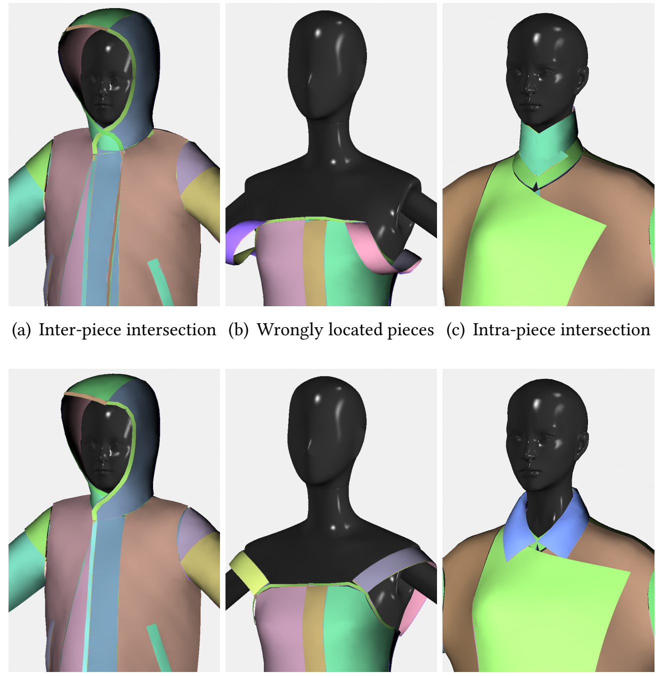

(a) Inter-piece intersection (b) Wrongly located pieces (c) Intra-piece intersection

(d) Inter-piece intersection fixed by user intervention (e) Wrongly located pieces fixed by user intervention (f) Intra-piece intersection fixed by user intervention

Fig. 9. Typical minor artifacts occurred to the garments initialized by our system. While all of them can be fixed by user intervention as shown in (d), (e), and (f), our implementation provides an option for users to fix inter-piece intersection only.

(a) Jogger pants (b) Business pants (c) Culotte pants (d) Skater dress (e) Mini dress

(f) Puff-sleeve dress (g) Structured mini dress (h) Tropical sundress (i) Slip dress (j) Pinafore dress

(k) Gingham shirt (l) Utility shirt (m) Puffer coat (n) Down coat (o) Trench coat

(p) Wrap coat (q) Cinched blazer (r) Color-block hoodie (s) Baby romper (t) Skater skirt

Fig. 10. The digital garments produced by a physics-based simulator following our initialization process. Note that our initialization excludes accessory details like zippers, buttons, and laces, as well as simulation specifics like filling and folding. These elements require additional user editing during or after simulation.